Hysteresis and mode coupling in capillary bridge oscillations: Observations

Wei Wei,* David B. Thiessen, and Philip L. Marston†
Department of Physics and Astronomy, Washington State University, Pullman, Washington 99164-2814, USA
(Received 31 May 2005; published 29 December 2005)

We investigate nonlinear axisymmetric oscillations of capillary bridges in a Plateau tank of density-matched liquids. The liquids are selected to have unusually small kinematic viscosities. Large amplitude oscillations are excited by applying oscillating Maxwell stresses. The modal frequency response is measured by incrementing the excitation frequency. In a narrow range of frequencies the response depends on the direction (downward or upward) of the increments in a way consistent with a lumped-parameter model of hysteresis for weakly damped oscillators having a mode-softening nonlinearity. The bridge length is selected so that the third harmonic is the natural frequency of a higher-order capillary mode and that mode also exhibits hysteresis.

DOI: 10.1103/PhysRevE.72.067304 PACS number(s): 05.45.−a, 81.70.Ha, 47.55.Dz

The dynamics of capillary bridges and closely related surface tension dominated fluidic systems have been investigated for over 150 years [1,2]. Cylindrical bridges between two solid supports have been investigated because of diverse applications and because of the subtleties of the stability and dynamics of bridges [1–13]. The dynamics of a nearly cylindrical liquid bridge is strongly influenced by the length of the bridge. In the absence of body forces, capillarity usually causes varicose perturbations of cylindrical liquid columns to become unstable when the perturbation wavelength exceeds the circumference [1,2,13,14]. This Rayleigh-Plateau instability has been suppressed by using electrostatic or acoustic surface stresses to modify the low-amplitude dynamics of bridges [11,15,16]. The oscillatory dynamics of finite amplitude perturbations is predicted to be complicated by nonlinear hysteresis [9] and mode coupling [10]. Such complications will be important for anticipating the responses of capillary systems to vibration [3–12]. Experiments on the oscillatory dynamics of capillary bridges having negligible body forces are ordinarily hampered by the limited duration of rocket or aircraft-based low effective-gravity platforms [7,15,16] or by complications introduced by forming the bridge in a Plateau tank of density matched immiscible liquids [4,11,12]. Viscous dissipation of modes is much greater for Plateau tank bridges than for bridges in air. The short duration of low-gravity measurements and the enhanced dissipation in Plateau tanks make it difficult to investigate nonlinear hysteretic behavior [9]. We show here that with a suitable choice of Newtonian liquids, dissipation in a Plateau tank can be reduced sufficiently to facilitate direct observation of hysteresis and nonlinear coupling of bridge modes. While mode-softening hysteretic capillary oscillations of pendant [17,18] and levitated [19] drops have been previously reported, our observations of hysteretic capillary oscillations appear to be the first describable by an elementary lumped-parameter model [20]. The dynamical region examined here is intermediate between the domains of linear analysis and capillary pinch off [21].

Bridge modes are designated by (n,m) where n denotes the number of axial half wavelengths and m is an azimuthal index that is zero for varicose modes [11,12]. The slenderness of the bridge is designated by $S=L/2R$ where L is the bridge length and R is the support radius, which corresponds to the static bridge radius for an ideal bridge. Figure 1 shows the shapes of the (3,0) and (5,0) modes computed for $S=2.71$, which is the slenderness value used in our experiments. These shapes are computed from a linearized inviscid model [4] where, as in our experiments, the contact lines are pinned to a disk of radius R at each end. Nicholas and Vega [9] predict that as a consequence of nonlinearity, nearly inviscid liquid bridges subjected to axial vibrations will exhibit a hysteresis in the response of the (2,0) mode. In the experiments described here, the (3,0) mode of an electrically conducting horizontal liquid bridge is excited using oscillating electrostatic fields instead of by vibrating either disk.

It is convenient to use a lumped-parameter model of weakly nonlinear bridge oscillations generalized from the Duffing model commonly used for the (2,0) mode [5–7]. As explained below, we have selected the slenderness S such that the amplitudes of the (3,0) and (5,0) modes are significantly coupled. The corresponding instantaneous amplitudes are denoted by $x(t)$ and $y(t)$, respectively, where t denotes the time. The profile and frequency of the applied stress are such that the (5,0) mode is weakly excited in comparison to the (3,0) mode and all modes having $m \neq 0$ have negligible amplitudes. Considering the symmetry of the (3,0) and (5,0) modes, when y is small the important terms of the potential energy related to the deformation of the bridge should have the form

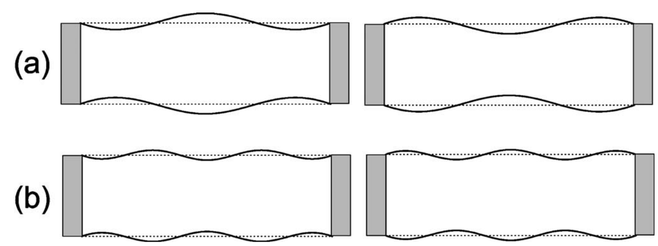

FIG. 1. (a) The (3,0) mode shape and its shape after half of its oscillation period. (b) The (5,0) mode shape and its shape after half of its oscillation period. These are computed from Sanz [4].

*Present address: Apt. E103, 7711 NE 175th St., Kenmore WA 98028.
†Electronic address: marston@wsu.edu

$$U=(1/2)k_3x^2+(1/3)\alpha_3x^3+(1/4)\beta_3x^4+\delta_{35}x^3y+(1/2)k_5y^2, \tag{1}$$

where k_3 and k_5 are modal spring coefficients, $\beta_3<0$ and α_3 are coefficients related to softening of the (3,0) mode and δ_{35} is a mode coupling term. Neglecting a term $\propto\delta_{35}x^3y$ since y is small, the modal restoring force for the (3,0) mode becomes $F_x=-k_3x-\alpha_3x^2-\beta_3x^3$. When the bridge is driven with an external modal stress at a frequency ω the modal equation becomes

$$x_{tt}+2\Gamma x_t+\omega_3^2x=-\alpha x^2-\beta x^3+f_E\cos\omega t, \tag{2}$$

where f_E is proportional to the external drive, ω_3 is the infinitesimal amplitude natural frequency, Γ is the damping, $\alpha=\alpha_3/M_3$, $\beta=\beta_3/M_3$, where M_3 is the modal mass of the (3,0) mode. The analogous expression for the (2,0) mode omits the term proportional to α as a consequence of the mode symmetry [5–7]. As with the (2,0) mode, the (3,0) mode is expected to soften at large amplitudes so that $\beta<0$. The resulting steady-state amplitude b of the (3,0) mode is [20]

$$b^2[(\epsilon-\kappa b^2)^2+\Gamma^2]=f_E^2/4\omega_3^2, \tag{3}$$

where $\kappa=(3\beta/8\omega_3)-(5\alpha^2/12\omega_3^3)$, $\epsilon=\omega-\omega_3$, and it is assumed that $(\Gamma/\omega_3)^2\ll 1$ so that a damping correction to the mode frequency is negligible. A feature of this cubic equation in b^2 is that when Γ is small, there is a range of frequencies in which two different stable b are possible. The amplitude at which the bridge vibrates in this range depends on the direction of approach. The amplitude equation derived by Nicolas and Vega for the (2,0) mode also predicts hysteresis, Eq. (4.12) of Ref. [9]. It may be recast as Eq. (3) by grouping the parameters appropriately. In that analysis, however, ϵ is modified to include weak aspects of inertia and damping neglected in (3). We include the most significant of those corrections by obtaining ω_3 with a fitting procedure.

For the (5,0) mode, the restoring force obtained from Eq. (1) is

$$F_y=-k_5y-\delta_{35}x^3. \tag{4}$$

When the (3,0) mode is driven at frequency ω, from the identity $4\cos^3\omega t=\cos 3\omega t+3\cos\omega t$, there will be a third harmonic response in the (5,0) mode amplitude y and that response is proportional to b^3. In our experiment we have selected S such that the radian frequency ω_5 of the (5,0) mode of an inviscid bridge is $\approx 3\omega_3$. This was done to enhance the magnitude of y. We find from Ref. [4] that for an inviscid bridge, the condition $\omega_5=3\omega_3$ gives $S=2.682$. To promote mode conversion this condition need not be satisfied exactly because the (5,0) resonance is relatively broad. Mancebo *et al.* [10] give other conditions for enhancing mode conversion by selecting S such that various ω_n differ by factors of 2.

This Plateau tank was previously used to investigate active damping of the (2,0) mode [12]. The liquids were selected such that the kinematic viscosities ν_i and ν_o of the bridge and bath liquids are small (0.62 cS and 0.77 cS). The bridge liquid (an aqueous solution of 52 wt. % CsCl) is electrically conducting and is grounded. The bath liquid (HFE-7500 from 3*M*) is an electrical insulator. The disk radius R is 3.18 mm and the Ohnesorge number (a reciprocal of a Reynolds number) is small, $C=\nu_i(\rho/\sigma R)^{1/2}=0.0024$ where $\rho=1.61$ g/cm^3 and $\sigma=33.6$ dyn/cm is the interfacial tension. Potentials are applied to an array of annular disk electrodes in such a way that the modal Maxwell stress on a cylindrical bridge has a sinusoidal time dependence of frequency $f=\omega/2\pi$. This is facilitated with an analog square-root circuit and related components [11,12]. Our previous electrode configuration [12] was modified to favor the excitation of the (3,0) mode. This was achieved by using three electrodes. At the middle of the bridge is an electrode of inner radius $a_1=7.4$ mm. An electrode is placed at $L/6$ from each end having an inner radius $a_2=9.1$ mm. The dimensions were selected in such a way that the gap ratio $(a_2-R)/(a_1-R)\approx\sqrt{2}$ so that for electrode potentials of the same magnitude, the Maxwell stress from the middle electrode is approximately twice that from either outer electrode. The ratio a_2/R was selected in such a way that the Maxwell stress distribution associated with a single electrode couples effectively to the mode of interest [11]. The time dependence of potentials is the special case of "no feedback" for our previously described system [11,16]. The middle electrode is activated (grounded) when the outer two are grounded (activated). The peak electrode voltage is 900 V. The electric field at the bridge's surface near an activated electrode is proportional to $\sqrt{|\cos\omega t|}$ giving a local stress proportional to $|\cos\omega t|$. By activating or grounding electrodes only when the field vanishes, the modal force is proportional to $\cos\omega t$ as in Eq. (2) [11]. To change ω without disturbing the bridge dynamics, the input to the square-root circuit was synthesized to be proportional to $\cos[\varphi(t)]$ where φ is an increasing continuous function of time with $d\varphi/dt$ bounded by the initial and final ω of each transition.

The response of the bridge is measured over the range 4.0 Hz to 3.3 Hz by first incrementally decreasing the drive frequency f and waiting 60 s for the bridge oscillations to achieve steady amplitude. The magnitude of the potential oscillations applied to the electrodes is held fixed. Then the oscillations are recorded with a 200 frames/s digital video camera and f is decreased to the next value. Larger increments were selected away from the (3,0) resonance so as to minimize drift of the bridge properties by reducing the amount of time required to complete the scan. This is followed immediately by an upward scan in which the same frequency set is used. During the downward scan the response initially increases, followed by an abrupt decrease, and then a gradual decrease. During the upward scan there is a sudden upward jump in the response at a frequency above that of the aforementioned downward jump. These are the features expected of a system with mode-softening hysteresis [9,17–20]. Figures 2 and 3 show image sequences of bridge oscillations obtained in this way with $f=3.51$ Hz during the downward and upward sweeps, respectively. The amplitude in Fig. 3 is significantly smaller than in Fig. 2. The bridge volume was $0.99\ \pi R^2L$ with $S=L/2R=2.71$.

For each f the modal response was obtained by analyzing 600 recorded images (512×216 pixels). Let z denote the

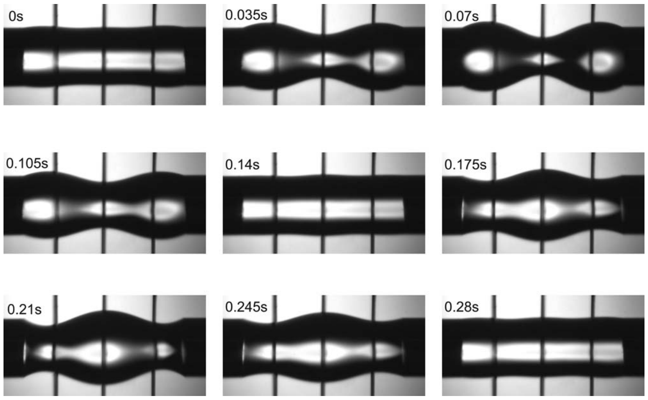

FIG. 2. Picture sequence of the bridge oscillations at a steady frequency f of 3.51 Hz. This f was approached from above.

axial coordinate of the bridge. For the image recorded at time t of a given sequence, the local diameter $d(z,t)$ was expanded using basis functions $F_n(z)$

$$d(z,t)/2 = r_0 + \sum_{n=2}^{11} c_n(t)F_n(z), \tag{5}$$

where the $F_n(z)$ are proportional to the mode shape functions of Sanz [4], normalized so that for each n the maximum $F_n=1$. For odd n, $F_n=1$ at the center of the bridge. The $c_n(t)$ and r_0 were determined by minimizing the rms error and r_0 has the same value for each sequence; $c_n(t)$ were expanded as $a_{n0}+a_{n1}\cos(\omega t+\phi_{n1})+a_{n2}\cos(2\omega t+\phi_{n2})+a_{n3}\cos(3\omega t+\phi_{n3})$, $\omega=2\pi f$, to obtain the dominant spectral components. The a_{nj} and ϕ_{nj} were determined by minimizing the rms error. The bridge response was predominantly from the a_{31} term as suggested by comparison of Figs. 2 and 3 with Fig. 1. The measures used for the spectral components of $x(t)$ and $y(t)$ at f and $3f$ are $b=a_{31}$ and $Y=a_{53}$, respectively. The resulting values of b/R and Y/R are plotted as points in Figs. 4 and 5. The measured b and Y exhibit hysteresis for f of 3.50, 3.51, and 3.52 Hz.

Measured b/R were compared with the predictions of the lumped-parameter model, Eq. (3). It was necessary to use fitted parameters because there is no complete hydrodynamic model of Plateau tank bridges, even in the linearized case. This approach is used although some related two-liquid problems have been analyzed using the full Navier-Stokes equations [21]. The approach used here avoids complications associated with oscillating boundary layers close to the bridge and perturbations in the flow of the outer liquid resulting from flow around the electrodes. The four parameters are $\omega_3=2\pi f_3$, Γ, κ, and f_E. The curve in Fig. 4 is given by adjusting these parameters to minimize the error. The parameters give $f_3=3.800$ Hz, $\Gamma=0.842$ s^{-1}, $\kappa/R^2=-1792$ s^{-2}, and

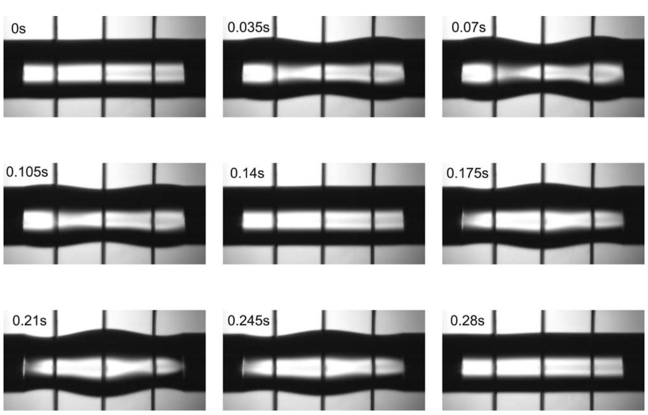

FIG. 3. Picture sequence of the bridge oscillations at a steady frequency f of 3.51 Hz. This f was approached from below. The amplitude is lower than in Fig. 2.

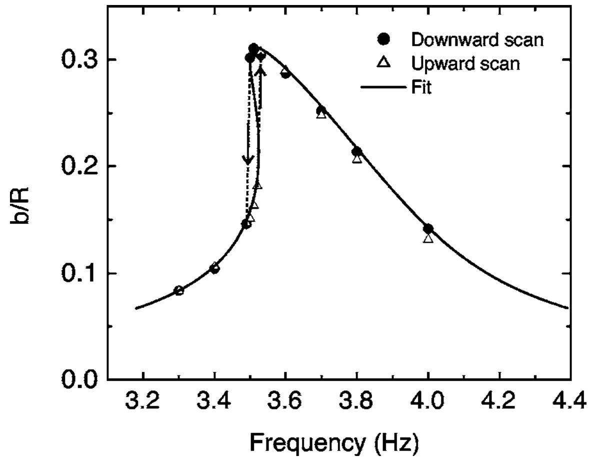

FIG. 4. Response of the bridge (3,0) mode at the driving frequency f. The oscillation amplitude is normalized with respect to the bridge radius R. Solid circles are measured for the downward scan when the driving frequency is incremented from 4.0 Hz to 3.3 Hz. Open triangles are the upward scan results when the frequency is incremented from 3.3 Hz to 4.0 Hz. The curve is a lumped parameter model, Eq. (3), with a four-parameter fit. The dotted lines and the associated arrows show the observed sudden transitions.

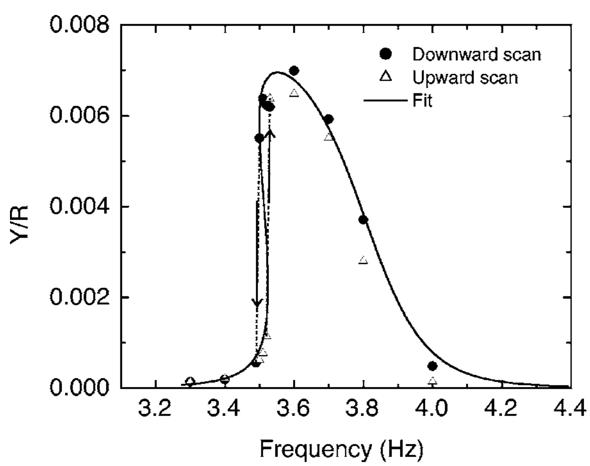

FIG. 5. Response of the bridge (5,0) mode at frequency $3f$ plotted as a function of f for the scans shown in Fig. 4. The oscillation amplitude is normalized with respect to R. Solid circles are measured for the downward scan. Open triangles are from the upward scan. The curve is a lumped parameter model, Eq. (6), that uses two additional fitted parameters. The dotted lines and the associated arrows show the observed sudden transitions.

$f_E/R=12.51\ \mathrm{s}^{-2}$. The model recovers the abrupt transitions in the hysteretic region. The assumption in Eq. (2) that $Y \ll b$ is consistent with our observations.

Two additional parameters are needed to model the (5,0) mode amplitude. These are the (5,0) mode damping Γ_5 and a normalized coupling $\delta=\delta_{35}/M_5$ where M_5 is a modal mass. Restricting attention to the response at 3ω from the coupling term in Eq. (4) gives

$$Y = (b^3|\delta|/8\omega_5)/\sqrt{[\Gamma_5^2 + (\omega_5 - 3\omega)^2]}, \qquad (6)$$

where $\omega_5=3\omega_3$ and a small resonance shift of order $(\Gamma_5/\omega_5)^2$ is neglected as in Eq. (26.7) of Ref. [20]. The curve in Fig. 5 is given by taking b from the curve in Fig. 4 and using fitted values of $|\delta|$ and Γ_5. The fit gives $\Gamma_5=3.96\ \mathrm{s}^{-1}$ and $|\delta|R^2/\Gamma_5=54.39$. Again the model recovers the abrupt transitions in the hysteretic region. Compared to the peak amplitude, the transitions are larger than in Fig. 4 because of the dependence on b^3. Attempts were unsuccessful to explain this behavior by mechanisms resulting from the weak modulation of the Maxwell stress associated with (3,0) mode oscillations since the resulting contributions to Y scale in a way inconsistent with observations. The enhanced spread in the measurements in Fig. 5 when $f \geq 3.6$ Hz may be only partially associated with variations in the measured b and the b^3 scaling. Small drifts in the properties of the (5,0) mode may also be relevant. Attempts to reduce the drifts in measurements of b and Y to below the range shown in Figs. 4 and 5 were unsuccessful. Profiles of the static bridge prior to and following the scans indicate that the Bond number $B=(\rho_i-\rho_o)gR^2/\sigma$ (where $g=9.8\ \mathrm{m/s^2}$) had drifted from -0.007 to 0.004 at the end. This drift appears to be associated with prolonged large amplitude bridge excitation. The hysteresis was verified for several different bridges and was not caused by the drift in B.

The observations in Fig. 4 suggest that liquid bridges subjected to sufficiently narrow-bandwidth ambient vibrations may exhibit hysteresis if the damping is small and the vibration amplitude is large. Mancebo *et al.* [10] predict that mode coupling from (and to) the (6,0) mode of weakly damped bridges having a slenderness $S \approx 2.23$ can result in chaotic oscillations. Though we find no evidence of chaotic motion in bridges with $S=2.71$, our observations of hysteresis and mode coupling are suggestive that chaotic oscillations are plausible if other modes and a wide range of excitation conditions could be investigated. In addition to the x^3y contribution to the potential energy U, where $x(t)$ and $y(t)$ correspond, respectively, to the instantaneous amplitudes of the (3,0) and (5,0) modes, it is plausible that the conversion to the (5,0) mode at the third harmonic of the excitation may be influenced by advective nonlinearities not considered here. It is also plausible that weakly nonlinear hysteretic and mode coupling responses of other capillary systems may be describable by elementary lumped parameter models, however the selection of the relevant contributions to the potential energy will depend on the symmetry and boundary conditions of the specific system.

This research was supported by NASA.

[1] J. Eggers, Rev. Mod. Phys. **69**, 865 (1997).
[2] J. Plateau, Ann. Phys. Chem. **80**, 566 (1850).
[3] M. P. Mahajan, M. Tsige, S. Y. Zhang, J. I. D. Alexander, P. L. Taylor, and C. Rosenblatt, Phys. Rev. Lett. **84**, 338 (2000).
[4] A. Sanz, J. Fluid Mech. **156**, 101 (1985).
[5] D. Rivas and J. Meseguer, J. Fluid Mech. **138**, 417 (1984).
[6] J. M. Perales and J. Meseguer, Phys. Fluids A **4**, 1110 (1992).
[7] I. Martinez, J. M. Perales, and J. Meseguer, Exp. Fluids **37**, 775 (2004).
[8] D. J. Mollot, J. Tsamopoulos, T. -Y. Chen, and N. Ashgriz, J. Fluid Mech. **255**, 411 (1993).
[9] J. A. Nicolás and J. M. Vega, J. Fluid Mech. **328**, 95 (1996).
[10] F. J. Mancebo, J. A. Nicolás, and J. M. Vega, Phys. Fluids **10**, 1088 (1998).
[11] M. J. Marr-Lyon, D. B. Thiessen, F. J. Blonigen, and P. L. Marston, Phys. Fluids **12**, 986 (2000).
[12] W. Wei, D. B. Thiessen, and P. L. Marston, Phys. Fluids **17**, 032105 (2005).
[13] B. J. Lowry and P. H. Steen, Proc. R. Soc. London, Ser. A **449**, 411 (1995).
[14] J. C. Maxwell to W. Thomson, Letter dated August 2, 1857 reproduced in S. G. Brush, C. W. F. Everitt, and E. Garber, *Maxwell on Saturn's rings* (MIT Press, Cambridge, MA, 1983), pp. 44–48.
[15] M. J. Marr-Lyon, D. B. Thiessen, and P. L. Marston, Phys. Rev. Lett. **86**, 2293 (2001).
[16] D. B. Thiessen, M. J. Marr-Lyon, and P. L. Marston, J. Fluid Mech. **457**, 285 (2002).
[17] D. W. DePaoli, J. Q. Feng, O. A. Basaran, and T. C. Scott, Phys. Fluids **7**, 1181 (1995).
[18] E. D. Wilkes and O. A. Basaran, J. Fluid Mech. **393**, 333 (1999).
[19] E. H. Trinh, R. G. Holt, and D. B. Thiessen, Phys. Fluids **8**, 43 (1996).
[20] L. D. Landau and E. M. Lifshitz, *Mechanics* (Pergamon, New York, 1960), pp. 77–91.
[21] P. Doshi, I. Cohen, W. W. Zhang, M. Siegel, P. Howell, O. A. Basaran, and S. R. Nagel, Science **302**, 1185 (2003).